Document Version
Peer reviewed version

Multi-Tenant C-RAN With Spectrum Pooling: Downlink Optimization Under Privacy Constraints

Seok-Hwan Park, *Member*, *IEEE*, Osvaldo Simeone, *Fellow, IEEE*,

and Shlomo Shamai (Shitz), *Fellow, IEEE*

arXiv:1710.06094v1 [cs.IT] 17 Oct 2017

Abstract

Spectrum pooling allows multiple operators, or tenants, to share the same frequency bands. This work studies the optimization of spectrum pooling for the downlink of a multi-tenant Cloud Radio Access Network (C-RAN) system in the presence of inter-tenant privacy constraints. The spectrum available for downlink transmission is partitioned into private and shared subbands, and the participating operators cooperate to serve the user equipments (UEs) on the shared subband. The network of each operator consists of a cloud processor (CP) that is connected to proprietary radio units (RUs) by means of finite-capacity fronthaul links. In order to enable inter-operator cooperation, the CPs of the participating operators are also connected by finite-capacity backhaul links. Inter-operator cooperation may hence result in loss of privacy. Fronthaul and backhaul links are used to transfer quantized baseband signals. Standard quantization is considered first. Then, a novel approach based on the idea of correlating quantization noise signals across RUs of different operators is proposed to control the trade-off between distortion at UEs and inter-operator privacy. The problem of optimizing the bandwidth allocation, precoding, and fronthaul/backhaul compression strategies is tackled under constraints on backhaul and

fronthaul capacity, as well as on per-RU transmit power and inter-operator privacy. For both cases, the optimization problems are tackled using the concave convex procedure (CCCP), and extensive numerical results are provided.

Index Terms

C-RAN, multi-tenant, spectrum pooling, RAN sharing, privacy constraint, precoding, fronthaul compression, multivariate compression.

I. INTRODUCTION

Spectrum pooling among multiple network operators, or tenants, is an emerging technique for meeting the rapidly increasing traffic demands over the available scarce spectrum resources [1]-[6]. Spectrum pooling can be implemented by means of orthogonal or non-orthogonal resource allocation. In orthogonal spectrum pooling, the frequency channels are exclusively, but dynamically, allocated to the participating operators [2]. In contrast, with non-orthogonal spectrum pooling, parts of the spectrum can be shared between operators. In addition to spectrum pooling, radio access network (RAN) sharing, whereby RAN infrastructure nodes are shared by the tenants, has also been considered [4][5]. RAN sharing and spectrum pooling are two examples of network slicing, a key technology for the upcoming 5G wireless systems [3][7].

In a Cloud RAN (C-RAN) architecture, a Cloud Processor (CP) carries out centralized baseband signal processing on behalf of a number of the connected Radio Units (RUs). The CP communicates quantized baseband signals over fronthaul links, while the RUs only perform radio frequency functionalities [8][9]. Motivated by the promised reduction in capital and operational expenditures, the C-RAN technology is currently being deployed for testing. In this paper, we focus on the optimization of spectrum pooling across multiple tenants in a C-RAN architecture, as illustrated in Fig. 1.

Existing papers on C-RAN downlink optimization, such as [10]-[16], have focused on single-tenant systems. These works, and related references, study the design of coordinated precoding and fronthaul compression strategies. Specifically, references [10][15][16] consider the use of standard point-to-point fronthaul compression and quantization strategies, whereas [11][12][14] investigate a more advanced approach based on multivariate compression and quantization. These perform the joint compression and quantization of baseband signals across multiple RUs, with the aim of controlling the impact of quantization distortion at the user equipments (UEs). Dual
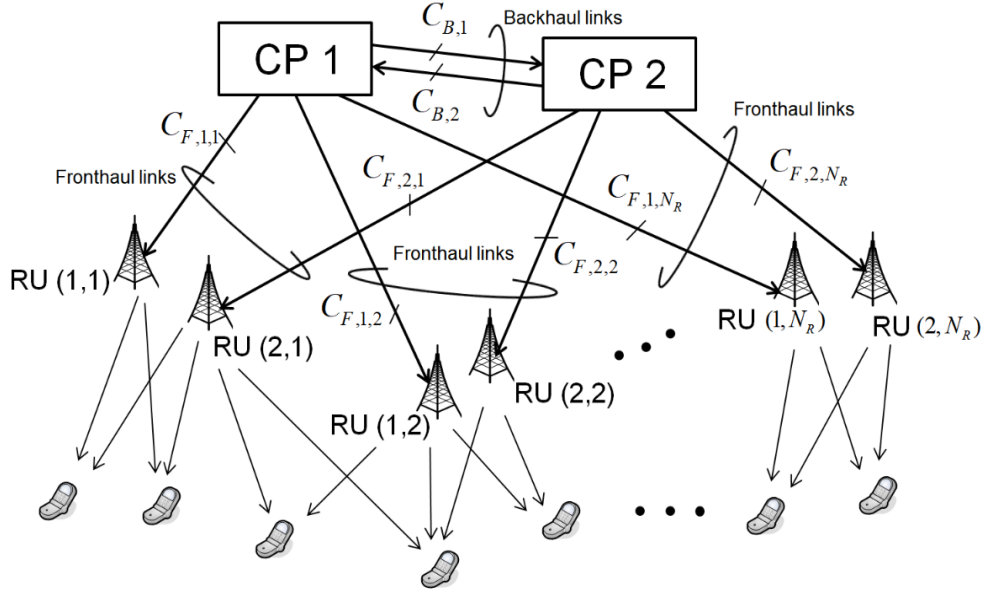
Figure 1. Illustration of the downlink of a multi-tenant C-RAN system.

approaches for the uplink of C-RAN were studied in, e.g., [17][18]. We refer to [8][9] for a comprehensive review.

Tackling the optimization of C-RAN systems in the presence of multiple operators presents novel optimization degrees of freedom and technical challenges. As a key novel design dimension, the available bandwidth may be optimally split into private and shared subbands, where the private subbands are exclusively used by the respective operators while the shared subband is shared by all the participating operators (see Fig. 2). Furthermore, cooperation and coordination on the shared subband are facilitated by communication between the CPs, which requires the design of the signals exchanged on the inter-CP interface as a function of the inter-CP capacity. Finally, the optimization problem entails a trade-off between the benefits accrued from inter-operator cooperation and the amount of information exchanged about the respective users' data.

In this paper, we study the design of the mult-tenant C-RAN system illustrated in Fig. 1 under the assumption that fronthaul and inter-CP backhaul links carry quantized baseband signals. Note that this is the standard mode of operation for C-RAN CP-toRUs links. We tackle the joint optimization of bandwidth allocation and of precoding and quantization strategies under constraints on fronthaul and backhaul capacity and privacy for the inter-CP communications.

To this end, we first consider standard point-to-point quantization as in most prior work on C-

RAN. Then, a novel quantizatoin scheme based on multivariate compression [11][14] is proposed. Through this approach, the CP of an operator is able to correlate the quantization noise signals across the RUs of *both* operators, so as to better control the trade-off between the distortion observed by the UEs and inter-operator privacy. Note that the crucial element of inter-operator privacy was not present in prior works [11][12][14]. In this regard, we note that the CP and RUs of one operator act as untrusted relays for the other operators, and hence the proposed technique can also be applied for the relay channels with untrusted relays studied in [19][20]. The formulated optimization problems, albeit non-convex, can be tackled via the concave convex procedure (CCCP) upon rank relaxation [11][13].

The rest of the paper is organized as follows. The system model is described in Sec. II, and Sec. III presents the operation of the multi-tenant C-RAN system with spectrum pooling. We discuss the optimization of the multi-tenant C-RAN system in Sec. IV. The novel multivariate compression scheme is introduced in Sec. V. We provide numerical results that validate the advantages of optimized spectrum pooling and of multivariate compression in Sec. VI, and the paper is concluded in Sec. VII.

Some notations used throughout the paper are summarized as follows. The mutual information between the random variables X and Y is denoted as $I(X;Y)$, and $h(X|Y)$ denotes the conditional differential entropy of X given Y. We use the notation $\mathcal{CN}(\boldsymbol{\mu}, \mathbf{R})$ to denote the circularly symmetric complex Gaussian distribution with mean $\boldsymbol{\mu}$ and covariance matrix $\mathbf{R}$. The set of all $M \times N$ complex matrices is denoted by $\mathbb{C}^{M \times N}$, and $\mathrm{E}(\cdot)$ represents the expectation operator. The operation $(\cdot)^{\dagger}$ denotes Hermitian transpose of a matrix or vector.

II. SYSTEM MODEL

We consider the downlink of a multi-tenant C-RAN with N_O operators. As shown in Fig. 1, we focus on the case of $N_O = 2$ operators, but the treatment could be generalized for any N_O at the cost of a more cumbersome notation. We assume that each operator has a single CP, N_R RUs and N_U UEs. We denote the rth RU and the kth UE of the ith operator as RU (i, r) and UE (i, k), respectively. We consider a general MIMO set-up in which RU (i, r) and UE (i, k) have $n_{R,i,r}$ and $n_{U,i,k}$ antennas, respectively, and define the number $n_{R,i} \triangleq \sum_{r \in \mathcal{N}_R} n_{R,i,r}$ of total RU antennas of each operator. The sets of RU and UE indices for either operator are denoted as $\mathcal{N}_R \triangleq \{1, 2, \ldots, N_R\}$ and $\mathcal{N}_U \triangleq \{1, 2, \ldots, N_U\}$, respectively, while $\mathcal{N}_O \triangleq \{1, 2\}$ is the set of operator indices.

The CP of each operator i, indicated as CP i, has a message $M_{i,k} \in \{1, 2, \ldots, 2^{nR_{i,k}}\}$ to deliver to UE (i, k), where n is the coding block length, assumed to be sufficiently large, and $R_{i,k}$ denotes the rate of the message $M_{i,k}$ in bits per second (bit/s).

As in related works for C-RAN systems (see, e.g., [10]-[12]), we assume that CP i is connected to RU (i, r) by a *fronthaul link* of capacity $C_{F,i,r}$ bit/s. In addition, in order to enable inter-operator cooperation, we assume that, as suggested in [4], the CPs of two operators are connected to each other. Specifically, CP i can send information to the other CP $\bar{i}$ on a *backhaul link* of capacity $C_{B,i}$ bit/s, where $\bar{i}$ indicates $\bar{i} = 3 - i$, i.e., $\bar{1} = 2$ and $\bar{2} = 1$. We note that it would be generally useful to deploy interfaces between the RUs of different operators [4], but this work focuses on investigating the advantages of inter-CP connections only.

Inter-operator cooperation via RAN sharing, as enabled by the inter-CP backhaul links, may cause information leakage from one operator to the other, which may degrade the confidentiality of the UE messages. When designing the multi-tenant C-RAN system, we will hence impose privacy constraints such that the inter-operator information leakage rate does not exceed a given tolerable threshold value.

We assume flat-fading channel models, and divide the downlink bandwidth as shown in Fig. 2 into private and shared subbands. The signal $\mathbf{y}_{i,k}^{(i)} \in \mathbb{C}^{n_{U,i,k} \times 1}$ received by UE (i, k) on private subband i can be written as

$$\mathbf{y}_{i,k}^{(i)} = \sum_{r \in \mathcal{N}_R} \mathbf{H}_{i,k}^{i,r} \mathbf{x}_{i,r}^{(i)} + \mathbf{z}_{i,k}^{(i)}, \tag{1}$$

where $\mathbf{H}_{i,k}^{j,r} \in \mathbb{C}^{n_{U,i,k} \times n_{R,j,r}}$ represents the channel matrix from RU (j, r) to UE (i, k); $\mathbf{x}_{i,r}^{(i)} \in \mathbb{C}^{n_{R,i,r} \times 1}$ is the signal transmitted by RU (i, r) on the private subband i; and $\mathbf{z}_{i,k}^{(i)} \sim \mathcal{CN}(\mathbf{0}, \mathbf{I})$ denotes the additive noise. Similarly, the signal $\mathbf{y}_{i,k}^{(S)} \in \mathbb{C}^{n_{U,i,k} \times 1}$ received by UE (i, k) on the shared subband is given as

$$\mathbf{y}_{i,k}^{(S)} = \sum_{r \in \mathcal{N}_R} \mathbf{H}_{i,k}^{i,r} \mathbf{x}_{i,r}^{(S)} + \sum_{r \in \mathcal{N}_R} \mathbf{H}_{i,k}^{\bar{i},r} \mathbf{x}_{\bar{i},r}^{(S)} + \mathbf{z}_{i,k}^{(S)}, \tag{2}$$

where $\mathbf{x}_{i,r}^{(S)} \in \mathbb{C}^{n_{R,i,r} \times 1}$ is the signal transmitted by RU (i, r) on the shared subband; and $\mathbf{z}_{i,k}^{(S)} \sim \mathcal{CN}(\mathbf{0}, \mathbf{I})$ is the additive noise.

III. MULTI-TENANT C-RAN WITH SPECTRUM POOLING

In this section, we describe the operation of the multi-tenant C-RAN system with spectrum pooling and RAN infrastructure sharing by means of inter-CP connections.
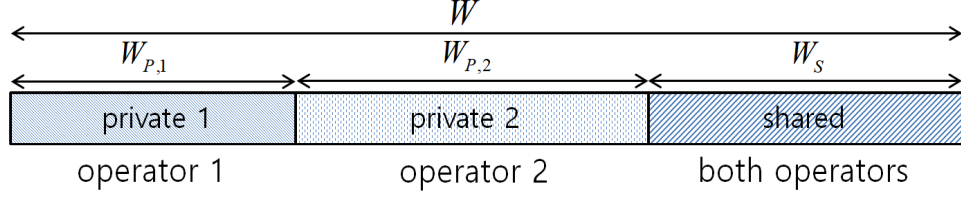
Figure 2. Illustration of frequency band splitting for the downlink transmission into private and shared bands.

A. Overview

As illustrated in Fig. 2, we split the frequency band of bandwidth W [Hz] into three subbands, where the first two subbands are exclusively used by the respective operators, while the last subband is shared by both operators. Accordingly, the bandwidth W is decomposed as

$$W = W_{P,1} + W_{P,2} + W_S, \tag{3}$$

where $W_{P,i}$ is the bandwidth of the private subband assigned to operator i, and W_S is the bandwidth of the shared subband.

The private subbands are used by each operator to communicate to their respective UEs with no interference from the other operators' RUs using standard fronthaul-enabled C-RAN transmission [8]. In contrast, the shared subband is used simultaneously by the two operators, which can coordinate their transmission through the inter-CP links. In the following, we detail the operation of CPs, RUs and UEs.

B. Encoding at CPs

In order to enable transmission over the private and shared subbands, we split the message $M_{i,k}$ intended for each UE (i, k) into two submessages $M_{i,k,P}$ and $M_{i,k,S}$ of rates $R_{i,k,P}$ and $R_{i,k,S}$, respectively, with $R_{i,k,P} + R_{i,k,S} = R_{i,k}$. The submessages $M_{i,k,P}$ and $M_{i,k,S}$ are communicated to the UE (i, k) on the private and shared subbands, respectively. Each submessage $M_{i,k,m}$, $m \in \{P, S\}$, is encoded by CP i in a baseband signal $\mathbf{s}_{i,k,m} \in \mathbb{C}^{d_{i,k,m} \times 1}$. We consider standard random coding with Gaussian codebooks, and hence each symbol $\mathbf{s}_{i,k,m}$ is distributed as $\mathbf{s}_{i,k,m} \sim \mathcal{CN}(\mathbf{0}, \mathbf{I})$.

1) Linear Precoding for Private Subband: CP i linearly precodes the signals $\{\mathbf{s}_{i,k,P}\}_{k \in \mathcal{N}_U}$ to be transmitted on the private subband as

$$\tilde{\mathbf{x}}_i^{(i)} = \left[\tilde{\mathbf{x}}_{i,1}^{(i)\dagger} \cdots \tilde{\mathbf{x}}_{i,N_R}^{(i)\dagger} \right]^\dagger = \sum_{k \in \mathcal{N}_U} \mathbf{V}_{i,k}^{(i)} \mathbf{s}_{i,k,P}, \tag{4}$$
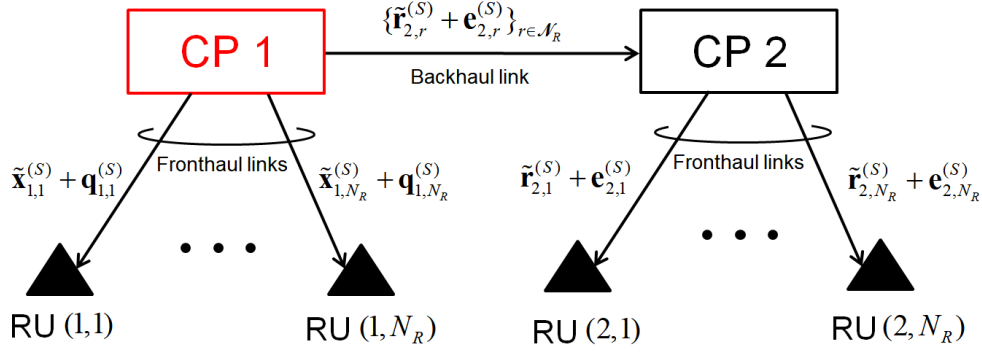
Figure 3. Illustration of fronthaul and backhaul quantization at CP 1.

where the subvector $\tilde{\mathbf{x}}_{i,r}^{(P)} \in \mathbb{C}^{n_{R,i,r} \times 1}$ is to be transferred to RU (i,r) on the fronthaul link, and $\mathbf{V}_{i,k}^{(i)} \in \mathbb{C}^{n_{R,i} \times d_{i,k,P}}$ is the precoding matrix for the signal $\mathbf{s}_{i,k,P}$.

2) Linear Precoding for Shared Subband: On the shared subband, the CPs and RUs of both operators are activated to cooperatively serve all the UEs. To this end, CP i precodes the signal $\mathbf{s}_{i,k,S}$ for each UE (i,k) into two precoded signals: signal $\tilde{\mathbf{x}}_i^{(S)} \in \mathbb{C}^{n_{R,i} \times 1}$ to be transmitted by its RUs and signal $\tilde{\mathbf{r}}_{\bar{i}}^{(S)} \in \mathbb{C}^{n_{R,\bar{i}} \times 1}$ to be sent by the other operator $\bar{i}$. This is illustrated in Fig. 3. As we will discuss, the transmission through the RUs of the other operator is enabled by the inter-CP backhaul link and is subject to privacy constraints.

Mathematically, we write the precoded signals in the shared subband as

$$\tilde{\mathbf{x}}_i^{(S)} = \left[\tilde{\mathbf{x}}_{i,1}^{(S)\dagger} \cdots \tilde{\mathbf{x}}_{i,N_R}^{(S)\dagger} \right]^{\dagger} = \sum_{k \in \mathcal{N}_U} \mathbf{V}_{i,k}^{(S)} \mathbf{s}_{i,k,S}, \tag{5}$$

$$\tilde{\mathbf{r}}_{\bar{i}}^{(S)} = \left[\tilde{\mathbf{r}}_{\bar{i},1}^{(S)\dagger} \cdots \tilde{\mathbf{r}}_{\bar{i},N_R}^{(S)\dagger} \right]^{\dagger} = \sum_{k \in \mathcal{N}_U} \mathbf{T}_{\bar{i},k}^{(S)} \mathbf{s}_{i,k,S}, \tag{6}$$

where the subvectors $\tilde{\mathbf{x}}_{i,r}^{(S)} \in \mathbb{C}^{n_{R,i,r} \times 1}$ and $\tilde{\mathbf{r}}_{\bar{i},r}^{(S)} \in \mathbb{C}^{n_{R,\bar{i},r} \times 1}$ are communicated to the RUs (i,r) and $(\bar{i},r)$, respectively; and $\mathbf{V}_{i,k}^{(S)} \in \mathbb{C}^{n_{R,i} \times d_{i,k,S}}$ and $\mathbf{T}_{\bar{i},k}^{(S)} \in \mathbb{C}^{n_{R,\bar{i}} \times d_{i,k,S}}$ are the precoding matrices for the signal $\mathbf{s}_{i,k,S}$ associated with the RUs (i,r) and $(\bar{i},r)$, respectively.

3) Fronthaul Compression: CP i is directly connected to the RUs (i,r) in its network via fronthaul links. Therefore, following the standard C-RAN operation, the CP i quantizes the precoded signals $\tilde{\mathbf{x}}_{i,r}^{(i)}$ and $\tilde{\mathbf{x}}_{i,r}^{(S)}$ for transmission on the fronthaul link to RU (i,r) on private and shared subbands. Assuming vector quantization, we model the quantized signals $\hat{\mathbf{x}}_{i,r}^{(m)}$, $m \in \{i, S\}$, as

$$\hat{\mathbf{x}}_{i,r}^{(m)} = \tilde{\mathbf{x}}_{i,r}^{(m)} + \mathbf{q}_{i,r}^{(m)}, \tag{7}$$

where $\mathbf{q}_{i,r}^{(m)}$ represents the quantization noise. Adopting a Gaussian test channel as in [10]-[12], the quantization noise $\mathbf{q}_{i,r}^{(m)}$ is independent of the precoded signal $\tilde{\mathbf{x}}_{i,r}^{(m)}$ and distributed as $\mathbf{q}_{i,r}^{(m)} \sim \mathcal{CN}(\mathbf{0}, \boldsymbol{\Omega}_{i,r}^{(m)})$. We recall that a Gaussian test channel can be well approximated by vector lattice quantizers [21].

We first adopt standard point-to-point compression, whereby the signals $\{\tilde{\mathbf{x}}_{i,r}^{(m)}\}_{r \in \mathcal{N}_R, m \in \{i, S\}}$ for different RUs and subbands are compressed independently. A more sophisticated approach based on multivariate compression will be discussed in Sec. V. Accordingly, with point-to-point compression, the rate, in bit/s, needed to send $\hat{\mathbf{x}}_{i,r}^{(m)}$ to RU (i, r) is given as $W_{i,m} I(\tilde{\mathbf{x}}_{i,r}^{(m)}; \hat{\mathbf{x}}_{i,r}^{(m)})$ [22, Ch. 3], where the mutual information $I(\tilde{\mathbf{x}}_{i,r}^{(m)}; \hat{\mathbf{x}}_{i,r}^{(m)})$ can be written as

$$I(\tilde{\mathbf{x}}_{i,r}^{(m)}; \hat{\mathbf{x}}_{i,r}^{(m)}) = g_{i,r}^{(m)}(\mathbf{V}, \boldsymbol{\Omega}) \tag{8}$$

$$= \Phi\left(\sum_{k \in \mathcal{N}_U} \mathbf{K}\left(\mathbf{E}_{i,r}^{\dagger} \mathbf{V}_{i,k}^{(m)}\right), \boldsymbol{\Omega}_{i,r}^{(m)}\right).$$

Here we defined the functions

$$\Phi(\mathbf{A}, \mathbf{B}) = \log_2 \det(\mathbf{A} + \mathbf{B}) - \log_2 \det(\mathbf{B}), \tag{9}$$

and $\mathbf{K}(\mathbf{A}) = \mathbf{A}\mathbf{A}^{\dagger}$; the shaping matrix $\mathbf{E}_{i,r} \in \mathbb{C}^{n_{R,i} \times n_{R,i,r}}$ that has all-zero elements except the rows from $\sum_{q=1}^{r-1} n_{R,i,q} + 1$ to $\sum_{q=1}^{r} n_{R,i,q}$ which contains an identity matrix; and the notation $W_{i,m} = W_{P,i} \cdot 1(m = i) + W_S \cdot 1(m = S)$.

4) Backhaul Compression: As seen in Fig. 3, since there is no direct link between CP i and the RUs $(\bar{i}, r)$ of the other tenant, CP i sends the precoded signal $\tilde{\mathbf{r}}_{\bar{i},r}^{(S)}$ to the RU $(\bar{i}, r)$ through CP $\bar{i}$. The CP $\bar{i}$ forwards the received bit stream from CP i to RU $(\bar{i}, r)$. Since both the backhaul link from CP i to CP $\bar{i}$ and the fronthaul link from CP i to RU $(\bar{i}, r)$ have finite capacities, CP i quantizes the signal $\tilde{\mathbf{r}}_{\bar{i},r}^{(S)}$ to obtain the quantized signal

$$\mathbf{r}_{\bar{i},r}^{(S)} = \tilde{\mathbf{r}}_{\bar{i},r}^{(S)} + \mathbf{e}_{\bar{i},r}^{(S)}, \tag{10}$$

where $\mathbf{e}_{\bar{i},r}^{(S)}$ represents the quantization noise. Using the same quantization model discussed above, this is distributed as $\mathbf{e}_{\bar{i},r}^{(S)} \sim \mathcal{CN}(\mathbf{0}, \boldsymbol{\Sigma}_{\bar{i},r}^{(S)})$. As mentioned, we assume here the independent compression of the signals $\{\tilde{\mathbf{r}}_{\bar{i},r}^{(S)}\}_{r \in \mathcal{N}_R}$ for different RUs, so that the rate needed to convey each signal $\mathbf{r}_{\bar{i},r}^{(S)}$ is given as $W_S I(\tilde{\mathbf{r}}_{\bar{i},r}^{(S)}; \mathbf{r}_{\bar{i},r}^{(S)})$, with

$$I(\tilde{\mathbf{r}}_{\bar{i},r}^{(S)}; \mathbf{r}_{\bar{i},r}^{(S)}) = \gamma_{\bar{i},r}^{(S)}(\mathbf{T}, \boldsymbol{\Sigma}) \tag{11}$$

$$= \Phi\left(\sum_{k \in \mathcal{N}_U} \mathbf{K}\left(\mathbf{E}_{\bar{i},r}^{\dagger} \mathbf{T}_{\bar{i},k}^{(S)}\right), \boldsymbol{\Sigma}_{\bar{i},r}^{(S)}\right).$$

The capacity constraint for the backhaul link from CP i to CP $\bar{i}$ can be written as

$$\sum_{r \in \mathcal{N}_R} W_S \gamma_{\bar{i},r}^{(S)}(\mathbf{T}, \boldsymbol{\Sigma}) \leq C_{B,i}, \ i \in \mathcal{N}_O, \tag{12}$$

since the backhaul link needs to carry the baseband signals for all the RUs. Similarly, the capacity constraint for the fronhtaul link from CP i to RU (i, r) can be expressed as

$$\sum_{m \in \{i,S\}} W_{i,m} g_{i,r}^{(m)}(\mathbf{V}, \boldsymbol{\Omega}) + W_S \gamma_{i,r}^{(S)}(\mathbf{T}, \boldsymbol{\Sigma}) \leq C_{F,i,r}, \ i \in \mathcal{N}_O, \ r \in \mathcal{N}_R, \tag{13}$$

since the fronthaul link needs to support transmission of the signals for both private and shared subbands.

5) Power Constraints: The signals $\mathbf{x}_{i,r}^{(i)}$ and $\mathbf{x}_{i,r}^{(S)}$ transmitted by RU (i, r) on the private and shared subbands are given as $\mathbf{x}_{i,r}^{(i)} = \hat{\mathbf{x}}_{i,r}^{(i)}$ and $\mathbf{x}_{i,r}^{(S)} = \hat{\mathbf{x}}_{i,r}^{(S)} + \mathbf{r}_{i,r}^{(S)}$, respectively. We impose per-RU transmission power constraints as

$$W_{P,i} p_{i,r}^{(i)}(\mathbf{V}, \boldsymbol{\Omega}) + W_S p_{i,r}^{(S)}(\mathbf{V}, \mathbf{T}, \boldsymbol{\Omega}) \leq P_{i,r}, \ i \in \mathcal{N}_O, \ r \in \mathcal{N}_R, \tag{14}$$

where $P_{i,r}$ represents the maximum transmission power allowed for RU (i, r), and the functions $p_{i,r}^{(i)}(\mathbf{V}, \boldsymbol{\Omega}, \mathbf{W})$ and $p_{i,r}^{(S)}(\mathbf{V}, \mathbf{T}, \boldsymbol{\Omega}, \mathbf{W})$ measure the transmission powers per unit bandwidth on the private and shared subbands, respectively, as

$$p_{i,r}^{(i)}(\mathbf{V}, \boldsymbol{\Omega}, \mathbf{W}) \triangleq \mathrm{E} \left\| \mathbf{x}_{i,r}^{(i)} \right\|^2 \tag{15}$$

$$= \left(\sum_{k \in \mathcal{N}_U} \mathrm{tr}\left(\mathbf{K}\left(\mathbf{E}_{i,r}^{\dagger} \mathbf{V}_{i,k}^{(i)} \right) \right) + \mathrm{tr}\left(\boldsymbol{\Omega}_{i,r}^{(i)} \right) \right),$$

$$p_{i,r}^{(S)}(\mathbf{V}, \mathbf{T}, \boldsymbol{\Omega}, \mathbf{W}) \triangleq \mathrm{E} \left\| \mathbf{x}_{i,r}^{(S)} \right\|^2 \tag{16}$$

$$= \left(\begin{array}{c} \sum_{k \in \mathcal{N}_U} \mathrm{tr}\left(\mathbf{K}\left(\mathbf{E}_{i,r}^{\dagger} \mathbf{V}_{i,k}^{(S)} \right) \right) + \mathrm{tr}\left(\boldsymbol{\Omega}_{i,r}^{(S)} \right) \\ + \sum_{k \in \mathcal{N}_U} \mathrm{tr}\left(\mathbf{K}\left(\mathbf{E}_{i,r}^{\dagger} \mathbf{T}_{i,k}^{(S)} \right) \right) + \mathrm{tr}\left(\boldsymbol{\Sigma}_{i,r}^{(S)} \right) \end{array} \right).$$

C. Decoding at UEs and Achievable Rates

Each UE (i, k) decodes the the submessage $M_{i,k,P}$ transmitted on the private subband based on the received signal $\mathbf{y}_{i,k}^{(i)}$, while treating the interference signals as additive noise. Then, the maximum achievable rate $R_{i,k,P}$ of the submessage $M_{i,k,P}$ can be written as

$$R_{i,k,P} = W_{P,i} I(\mathbf{s}_{i,k,P}; \mathbf{y}_{i,k}^{(i)}), \tag{17}$$

where

$$I(\mathbf{s}_{i,k,P}; \mathbf{y}_{i,k}^{(i)}) = f_{i,k,P}(\mathbf{V}, \mathbf{\Omega}) \tag{18}$$

$$= \Phi\left(\mathbf{K}\left(\mathbf{H}_{i,k}^i \mathbf{V}_{i,k}^{(i)}\right), \sum_{l \in \mathcal{N}_U \setminus \{k\}} \mathbf{K}\left(\mathbf{H}_{i,k}^i \mathbf{V}_{i,l}^{(i)}\right) + \mathbf{H}_{i,k}^i \mathbf{\Omega}_i^{(i)} \mathbf{H}_{i,k}^{i\dagger} + \mathbf{I}\right).$$

Here we defined the channel matrix $\mathbf{H}_{i,k}^j = [\mathbf{H}_{i,k}^{j,1} \mathbf{H}_{i,k}^{j,2} \cdots \mathbf{H}_{i,k}^{j,N_R}]$ from all the RUs of operator j to UE (i,k), and the matrix $\mathbf{\Omega}_i^{(i)} = \mathrm{diag}(\mathbf{\Omega}_{i,1}^{(i)}, \ldots, \mathbf{\Omega}_{i,N_R}^{(i)})$.

In a similar manner, we assume that UE (i,k) decodes the submessage $M_{i,k,S}$ sent on the shared subband from the received signal $\mathbf{y}_{i,k}^{(S)}$ by treating the interference signals as noise, so that the maximum achievable rate $R_{i,k,S}$ is given as

$$R_{i,k,S} = W_S I(\mathbf{s}_{i,k,S}; \mathbf{y}_{i,k}^{(S)}), \tag{19}$$

with the mutual information $I(\mathbf{s}_{i,k,S}; \mathbf{y}_{i,k}^{(S)})$ given as

$$I(\mathbf{s}_{i,k,S}; \mathbf{y}_{i,k}^{(S)}) = f_{i,k,S}(\mathbf{V}, \mathbf{T}, \mathbf{\Omega}) \tag{20}$$

$$= \Phi\left(\mathbf{K}\left(\begin{array}{c} \mathbf{H}_{i,k}^i \mathbf{V}_{i,k}^{(S)} \\ +\mathbf{H}_{i,k}^{\bar{i}} \mathbf{T}_{\bar{i},k}^{(S)} \end{array}\right), \left(\begin{array}{c} \sum_{l \in \mathcal{N}_U \setminus \{k\}} \mathbf{K}\left(\mathbf{H}_{i,k}^i \mathbf{V}_{i,l}^{(S)} + \mathbf{H}_{i,k}^{\bar{i}} \mathbf{T}_{\bar{i},l}^{(S)}\right) \\ +\sum_{l \in \mathcal{N}_U} \mathbf{K}\left(\mathbf{H}_{i,k}^i \mathbf{T}_{i,l}^{(S)} + \mathbf{H}_{i,k}^{\bar{i}} \mathbf{V}_{\bar{i},l}^{(S)}\right) \\ +\mathbf{H}_{i,k}^i \mathbf{\Omega}_i^{(S)} \mathbf{H}_{i,k}^{i\dagger} + \mathbf{H}_{i,k}^i \mathbf{\Sigma}_i^{(S)} \mathbf{H}_{i,k}^{i\dagger} \\ +\mathbf{H}_{i,k}^{\bar{i}} \mathbf{\Omega}_{\bar{i}}^{(S)} \mathbf{H}_{i,k}^{\bar{i}\dagger} + \mathbf{H}_{i,k}^{\bar{i}} \mathbf{\Sigma}_{\bar{i}}^{(S)} \mathbf{H}_{i,k}^{\bar{i}\dagger} + \mathbf{I} \end{array}\right)\right),$$

where we defined the matrices $\mathbf{\Omega}_i^{(S)} = \mathrm{diag}(\mathbf{\Omega}_{i,1}^{(S)}, \ldots, \mathbf{\Omega}_{i,N_R}^{(S)})$ and $\mathbf{\Sigma}_i^{(S)} = \mathrm{diag}(\mathbf{\Sigma}_{i,1}^{(S)}, \ldots, \mathbf{\Sigma}_{i,N_R}^{(S)})$.

D. Privacy Constraints

As discussed, inter-operator cooperation on the shared subband requires the transmission of precoded and quantized signals $\{\mathbf{r}_{\bar{i},r}^{(S)}\}_{r \in \mathcal{N}_R}$ between CP i and CP $\bar{i}$ on the backhaul link. As a result, CP $\bar{i}$ can infer some information about the messages $\{M_{i,k,S}\}_{k \in \mathcal{N}_U}$ intended for the UEs (i,k), $k \in \mathcal{N}_U$ of the operator i. In order to ensure that this leakage of information is limited, one can design both the precoding matrices $\mathbf{T}$ and the quantization covariance matrices $\mathbf{\Sigma}$ under the information-theoretic privacy constraint

$$W_S I(\mathbf{s}_{i,k,S}; \{\mathbf{r}_{\bar{i},r}^{(S)}\}_{r \in \mathcal{N}_R}) \leq \Gamma_{\mathrm{privacy}}. \tag{21}$$

In (21), the mutual information $I(\mathbf{s}_{i,k,S}; \{\mathbf{r}^{(S)}_{\bar{i},r}\}_{r \in \mathcal{N}_R})$ measures the amount of the information that can be inferred about each signal $\mathbf{s}_{i,k,S}$ by the CP $\bar{i}$ of the other operator based on the observation of $\{\mathbf{r}^{(S)}_{\bar{i},r}\}_{r \in \mathcal{N}_R}$. This mutual information can be written as

$$I(\mathbf{s}_{i,k,S}; \{\mathbf{r}^{(S)}_{\bar{i},r}\}_{r \in \mathcal{N}_R}) = \beta_{i,k,S}\left(\mathbf{T}, \boldsymbol{\Omega}\right) \tag{22}$$

$$= \Phi\left(\mathbf{K}\left(\mathbf{T}^{(S)}_{\bar{i},k}\right), \sum_{l \in \mathcal{N}_U \backslash \{k\}} \mathbf{K}\left(\mathbf{T}^{(S)}_{\bar{i},l}\right) + \boldsymbol{\Sigma}^{(S)}_{\bar{i}}\right).$$

The condition (21) imposes that the amount of leaked information does not exceed a predetermined threshold value Γ_{privacy}. This value has a specific operational meaning according to standard information-theoretic results [23, Ch. 4, Problem 33]. In particular, a privacy level of Γ_{privacy} implies that, if a user receives at rate R (bit/s) on shared subband, a bit stream of rate $\min(\Gamma_{\text{privacy}}, R)$ can be received securely, while the remaining rate $(R - \Gamma_{\text{privacy}})^+$ (bit/s) can be eavesdropped by the other operator.

In ensuring the satisfaction of the privacy constraint (21), the quantization noise introduced by the fronthaul quantization plays an important role. In fact, the fronthaul quantization noise is instrumental in masking information about the UE messages at the cost of a more significant degradation of the signals received by the UEs. A more advanced quantization scheme will be considered in Sec. V.

IV. OPTIMIZATION OF MULTI-TENANT C-RAN

We aim at jointly optimizing the bandwidth allocation $\mathbf{W}$, the precoding matrices $\{\mathbf{V}, \mathbf{T}\}$ and the quantization noise covariance matrices $\{\boldsymbol{\Omega}, \boldsymbol{\Sigma}\}$, with the goal of maximizing the sum-rate $R_{\Sigma} \triangleq \sum_{i \in \mathcal{N}_O} \sum_{k \in \mathcal{N}_U} (R_{i,k,P} + R_{i,k,S})$ of all the UEs, under constraints on backhaul and fronthaul

capacity, per-RU transmit power and inter-operator privacy levels. The problem can be stated as

$$\underset{\mathbf{V},\mathbf{T},\boldsymbol{\Omega},\boldsymbol{\Sigma},\mathbf{W},\mathbf{R}}{\text{maximize}} \sum_{i\in\mathcal{N}_O} \sum_{k\in\mathcal{N}_U} (R_{i,k,P} + R_{i,k,S}) \tag{23a}$$

$$\text{s.t. } R_{i,k,P} \leq W_{P,i} f_{i,k,P}\left(\mathbf{V},\boldsymbol{\Omega}\right), \ i\in\mathcal{N}_O, \ k\in\mathcal{N}_U, \tag{23b}$$

$$R_{i,k,S} \leq W_S f_{i,k,S}\left(\mathbf{V},\mathbf{T},\boldsymbol{\Omega}\right), \ i\in\mathcal{N}_O, \ k\in\mathcal{N}_U, \tag{23c}$$

$$\sum_{r\in\mathcal{N}_R} W_S \gamma_{i,r}^{(S)}\left(\mathbf{T},\boldsymbol{\Sigma}\right) \leq C_{B,i}, \ i\in\mathcal{N}_O, \tag{23d}$$

$$\sum_{m\in\{i,S\}} W_{i,m} g_{i,r}^{(m)}\left(\mathbf{V},\boldsymbol{\Omega}\right) + W_S \gamma_{i,r}^{(S)}(\mathbf{T},\boldsymbol{\Sigma}) \leq C_{F,i,r}, \ i\in\mathcal{N}_O, \ r\in\mathcal{N}_R, \tag{23e}$$

$$W_S \beta_{i,k,S}\left(\mathbf{T},\boldsymbol{\Omega}\right) \leq \Gamma_{\text{privacy}}, \ i\in\mathcal{N}_O, \ k\in\mathcal{N}_U, \tag{23f}$$

$$W_{P,i} p_{i,r}^{(i)}\left(\mathbf{V},\boldsymbol{\Omega}\right) + W_S p_{i,r}^{(S)}\left(\mathbf{V},\mathbf{T},\boldsymbol{\Omega}\right) \leq P_{i,r}, \ i\in\mathcal{N}_O, \ r\in\mathcal{N}_R, \tag{23g}$$

$$W_{P,1} + W_{P,2} + W_S = W. \tag{23h}$$

In (23), constraints (23b)-(23c) follow from the achievable rates (17) and (19); (23d)-(23e) are the backhaul and fronthaul capacity constraints (12) and (13); (23f) is the inter-operator privacy constraint (21); (23g) is the per-RU transmit power constraint (14); and (23h) is the sum-bandwidth constraint (3).

Since the problem (23) is non-convex, we adopt a Successive Convex Approximation (SCA) approach to obtain an efficient local optimization algorithm. To this end, we equivalently rewrite the constraints (23b) and (23c) using the epigraph form as

$$\log R_{i,k,P} \leq \log W_{P,i} + \log t_{f,i,k,P}, \ i\in\mathcal{N}_O, \ k\in\mathcal{N}_U, \tag{24}$$

$$t_{f,i,k,P} \leq f_{i,k,P}\left(\mathbf{V},\boldsymbol{\Omega}\right), \ i\in\mathcal{N}_O, \ k\in\mathcal{N}_U, \tag{25}$$

$$\text{and } \log R_{i,k,S} \leq \log W_S + \log t_{f,i,k,S}, \ i\in\mathcal{N}_O, \ k\in\mathcal{N}_U, \tag{26}$$

$$t_{f,i,k,S} \leq f_{i,k,S}\left(\mathbf{V},\mathbf{T},\boldsymbol{\Omega}\right) \ i\in\mathcal{N}_O, \ k\in\mathcal{N}_U, \tag{27}$$

respectively. We note that the conditions (24) and (26) are difference-of-convex (DC) constraints (see, e.g., [11][13]), and that the conditions (25) and (27) can be converted into DC constraints by expressing them with respect to the variables $\tilde{\mathbf{V}}_{i,k}^{(i)} = \mathbf{V}_{i,k}^{(i)}\mathbf{V}_{i,k}^{(i)\dagger}$ and $\tilde{\mathbf{U}}_{i,k}^{(S)} = \mathbf{U}_{i,k}^{(S)}\mathbf{U}_{i,k}^{(S)\dagger}$ with $\mathbf{U}_{i,k}^{(S)} = [\mathbf{V}_{i,k}^{(S)\dagger} \ \mathbf{T}_{i,k}^{(S)\dagger}]^{\dagger}$. Similarly, the other non-convex constraints (23e)-(23g) can also be transformed into DC conditions by relaxing the non-convex rank constraints $\text{rank}(\tilde{\mathbf{V}}_{i,k}^{(i)}) \leq d_{i,k,P}$ and $\text{rank}(\tilde{\mathbf{U}}_{i,k}^{(S)}) \leq d_{i,k,S}$. As a result of these manipulations, we finally obtain the DC problem (31) reported in Appendix A.

Algorithm 1 CCCP algorithm for problem (31)

---

1. Initialize the variables $\tilde{\mathbf{V}}'$, $\tilde{\mathbf{U}}'$, $\mathbf{\Omega}'$, $\mathbf{\Sigma}'$, $\mathbf{W}'$ and $\mathbf{R}'$ to arbitrary feasible values that satisfy the constraints (31b) and (31r) and set $q = 1$.

2. Update the variables $\tilde{\mathbf{V}}''$, $\tilde{\mathbf{U}}''$, $\mathbf{\Omega}''$, $\mathbf{\Sigma}''$, $\mathbf{W}''$ and $\mathbf{R}''$ as a solution of the convex problem (32) in Appendix A.

3. Stop if a convergence criterion is satisfied. Otherwise, set $\tilde{\mathbf{V}}' \leftarrow \tilde{\mathbf{V}}''$, $\tilde{\mathbf{U}}' \leftarrow \tilde{\mathbf{U}}''$, $\mathbf{\Omega}' \leftarrow \mathbf{\Omega}''$, $\mathbf{\Sigma}' \leftarrow \mathbf{\Sigma}''$, $\mathbf{W}' \leftarrow \mathbf{W}''$ and $\mathbf{R}' \leftarrow \mathbf{R}''$ and go back to Step 2.

We tackle the obtained DC problem by deriving an iterative algorithm based on the standard CCCP approach [11][13]. The detailed algorithm is described in Algorithm 1. In our simulations, we used the CVX software [24] to solve the convex problem (32) (see Appendix A) at Step 2. After the convergence of the algorithm, we need to project the variables $\tilde{\mathbf{V}}_{i,k}^{(i)''}$ and $\tilde{\mathbf{U}}_{i,k}^{(S)''}$ onto the spaces of limited-rank matrices satisfying $\mathrm{rank}(\tilde{\mathbf{V}}_{i,k}^{(i)}) \leq d_{i,k,P}$ and $\mathrm{rank}(\tilde{\mathbf{U}}_{i,k}^{(S)}) \leq d_{i,k,S}$, respectively. Without claim of optimality, we use the standard approach of obtaining the variables $\tilde{\mathbf{V}}_{i,k}^{(i)}$ and $\tilde{\mathbf{U}}_{i,k}^{(S)}$ by including the $d_{i,k,P}$ and $d_{i,k,S}$ leading eigenvectors of the matrices $\tilde{\mathbf{V}}_{i,k}^{(i)''}$ and $\tilde{\mathbf{U}}_{i,k}^{(S)''}$, respectively, as columns.

V. MULTIVARIATE COMPRESSION

In this section, we propose a novel quantization approach for inter-CP communication that aims at controlling the trade-off between the distortion at the UEs and inter-operator privacy. The approach is based on multivariate compression, first studied for single-tenant systems in [11][14]. To highlight the idea, we focus on the case of single RU per operator, i.e., $N_R = 1$, but extensions follow in the same way, albeit at the cost of a more cumbersome notation.

The key idea is for each CP i to jointly quantize the precoded signals to be transmitted by the tenants' RUs. In so doing, one can better control the impact of the quantization noise on the UEs' decoders, while still ensuring a given level of privacy with respect to CP $\bar{i}$.

Mathematically, CP i produces the linearly precoded signals $\tilde{\mathbf{x}}_{i,1}^{(S)}$ and $\tilde{\mathbf{r}}_{\bar{i},1}^{(S)}$ according to (5) and (6), respectively, and obtains the quantized signals $\hat{\mathbf{x}}_{i,1}^{(S)} = \tilde{\mathbf{x}}_{i,1}^{(S)} + \mathbf{q}_{i,1}^{(S)}$ and $\mathbf{r}_{\bar{i},1}^{(S)} = \tilde{\mathbf{r}}_{\bar{i},1}^{(S)} + \mathbf{e}_{\bar{i},1}^{(S)}$ that are transferred to RUs $(i, 1)$ and $(\bar{i}, 1)$, respectively. With multivariate compression of the precoded signals $\tilde{\mathbf{x}}_{i,1}^{(S)}$ and $\tilde{\mathbf{r}}_{\bar{i},1}^{(S)}$, CP i can ensure that the quantization noise signals $\mathbf{q}_{i,1}^{(S)}$ and $\mathbf{e}_{\bar{i},1}^{(S)}$ have a correlation matrix $\mathbf{\Theta}_i^{(S)} = \mathrm{E}[\mathbf{q}_{i,1}^{(S)} \mathbf{e}_{\bar{i},1}^{(S)\dagger}]$. As a result, the effective quantization noise

signal that affects the received signal $\mathbf{y}_{j,k}^{(S)}$ of UE (j,k) on the shared subband is given as $\tilde{\mathbf{q}}_{j,k}^{(S)} = \mathbf{H}_{j,k}^i \mathbf{q}_{i,1}^{(S)} + \mathbf{H}_{j,k}^{\bar{i}} \mathbf{e}_{\bar{i},1}^{(S)}$, whose covariance matrix depends on the correlation matrix $\mathbf{\Theta}_i^{(S)}$ as

$$\mathrm{E}\left[\tilde{\mathbf{q}}_{j,k}^{(S)}\tilde{\mathbf{q}}_{j,k}^{(S)\dagger}\right] = \mathbf{G}_{j,k}^i \mathbf{\Lambda}_i \mathbf{G}_{j,k}^{i\,\dagger}, \tag{28}$$

where the matrix $\mathbf{\Lambda}_i$ represents the covariance matrix of the stacked quantization noise signals $[\mathbf{q}_{i,1}^{(S)\dagger}\, \mathbf{e}_{\bar{i},1}^{(S)\dagger}]^\dagger$ as

$$\mathbf{\Lambda}_i = \mathrm{E}\left[\begin{bmatrix} \mathbf{q}_{i,1}^{(S)} \\ \mathbf{e}_{\bar{i},1}^{(S)} \end{bmatrix} \begin{bmatrix} \mathbf{q}_{i,1}^{(S)\dagger} & \mathbf{e}_{\bar{i},1}^{(S)\dagger} \end{bmatrix}\right] = \begin{bmatrix} \mathbf{\Omega}_{i,1}^{(S)} & \mathbf{\Theta}_i^{(S)} \\ \mathbf{\Theta}_i^{(S)\dagger} & \mathbf{\Sigma}_{\bar{i},1}^{(S)} \end{bmatrix} \succeq \mathbf{0}. \tag{29}$$

Designing $\mathbf{\Theta}_i^{(S)}$ hence allows us to control the effective noise observed by the UE, while also affecting the inter-operator privacy constraint (21).

For the optimization under multivariate compression, it was shown in [22, Ch. 9] that correlating the quantization noise signals imposes the following additional constraint on the variables $t_{g,i,1,S}$ and $t_{\gamma,\bar{i},r,S}$ in the DC problem (31) detailed in Appendix A:

$$h(\hat{\mathbf{x}}_{i,1}^{(S)}) + h(\mathbf{r}_{\bar{i},1}^{(S)}) - h(\hat{\mathbf{x}}_{i,1}^{(S)}, \mathbf{r}_{\bar{i},1}^{(S)} | \tilde{\mathbf{x}}_{i,1}^{(S)}, \tilde{\mathbf{r}}_{\bar{i},1}^{(S)})$$
$$= \log_2 \det\left(\sum_{k\in\mathcal{N}_U} \tilde{\mathbf{E}}_{i,1}^\dagger \tilde{\mathbf{U}}_{i,k}^{(S)} \tilde{\mathbf{E}}_{i,1} + \mathbf{\Omega}_{i,1}^{(S)}\right) + \log_2 \det\left(\sum_{k\in\mathcal{N}_U} \bar{\mathbf{E}}_{i,1}^\dagger \tilde{\mathbf{U}}_{i,k}^{(S)} \bar{\mathbf{E}}_{i,1} + \mathbf{\Sigma}_{\bar{i},1}^{(S)}\right)$$
$$- \log_2 \det(\mathbf{\Lambda}_i) \leq t_{g,i,1,S} + t_{\gamma,\bar{i},r,S}. \tag{30}$$

The optimization under multivariate quantization is stated as the problem (31) in Appendix A with the constraint (30) added. We can handle the problem following Algorithm 1 since the added condition is a DC constraint.

VI. NUMERICAL RESULTS

In this section, we present numerical results that validate the performance of multi-tenant C-RAN systems with spectrum pooling in the presence of the proposed optimization and quantization strategies. We assume that the positions of the RUs and UEs are uniformly distributed within a circular area of radius 100 m. For given positions of the RUs and the UEs, the channel matrix $\mathbf{H}_{i,k}^{j,r}$ from RU (j,r) to UE (i,k) is modeled as $\mathbf{H}_{i,k}^{j,r} = \sqrt{\rho_{i,k}^{j,r}}\tilde{\mathbf{H}}_{i,k}^{j,r}$, where $\rho_{i,k}^{j,r} = 1/(1 + (D_{i,k}^{j,r}/D_0)^\alpha)$ represents the path-loss, $D_{i,k}^{j,r}$ is the distance between the RU (j,r) to UE (i,k), and the elements of $\tilde{\mathbf{H}}_{i,k}^{j,r}$ are independent and identically distributed (i.i.d.) as $\mathcal{CN}(0,1)$. In the simulation, we set $\alpha = 3$ and $D_0 = 50$ m. Except for Fig. 7, we focus on the point-to-point compression strategy studied in Sec. III and Sec. IV.
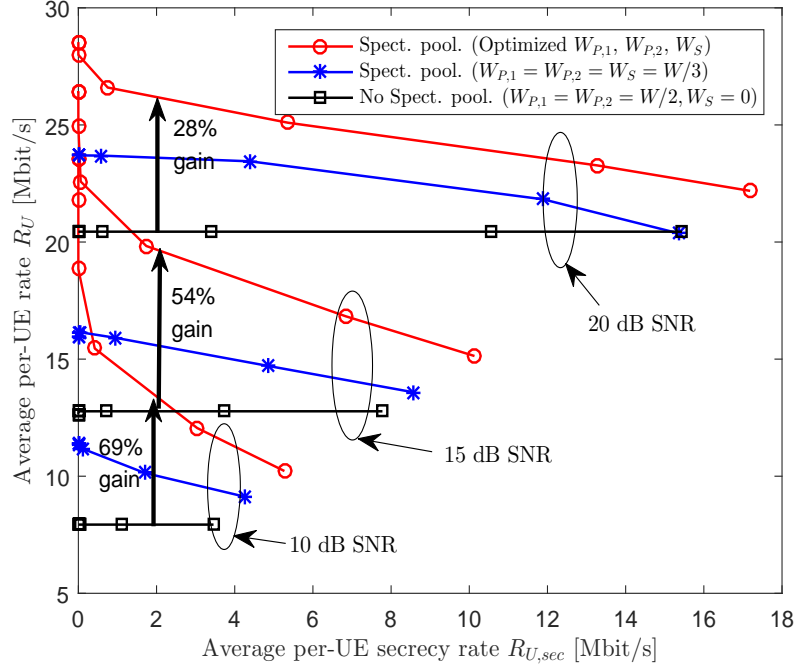
Figure 4. Average per-UE rate R_U versus average per-UE secrecy rate $R_{U,\text{sec}}$ ($N_R = N_U = 1$, $n_{R,i,r} = n_{U,i,k} = 1$, $C_{B,i} = 100$ Mbit/s, $C_{F,i,r} = 50$ Mbit/s and $W = 10$ MHz).

To validate the effectiveness of the proposed designs, we compare the following three schemes:

- *Spectrum pooling with optimized bandwidth allocation $W_{P,1}$, $W_{P,2}$ and W_S;*
- *Spectrum pooling with equal bandwidth allocation $W_{P,1} = W_{P,2} = W_S = W/3$;*
- *No spectrum pooling with equal bandwidth allocation $W_{P,1} = W_{P,2} = W/2$ and $W_S = 0$.*

The first approach adopts the proposed optimization algorithm (see Algorithm 1) discussed in Sec. IV. Instead, the other two baseline approaches are obtained by using the proposed algorithm with the added linear equality constraints $W_{P,1} = W_{P,2} = W_S = W/3$, or $W_{P,1} = W_{P,2} = W/2$ and $W_S = 0$, respectively. Except for the last scheme with no spectrum pooling, all schemes exhibit a trade-off between the achievable sum-rate and the guaranteed privacy level Γ_{privacy}. A smaller Γ_{privacy}, i.e., a stricter privacy constraint, generally entails a smaller sum-rate, and vice versa for a larger Γ_{privacy}. To quantify this effect, we define the per-UE secrecy rate $R_{U,\text{sec}}$ as $R_{U,\text{sec}} = [R_U - \Gamma_{\text{privacy}}]^+$, where R_U is the average per-UE achievable rate and $[\cdot]^+$ is defined as $[a]^+ = \max\{a, 0\}$. The rate R_U is given by the total sum-rate R_Σ divided by the number of total UEs, i.e., $R_U = R_\Sigma / (2N_U)$. Following the discussion in Sec. III-D, the quantity $R_{U,\text{sec}}$ measures the rate at which information is transmitted privately to each UE. In contrast, R_U represents the
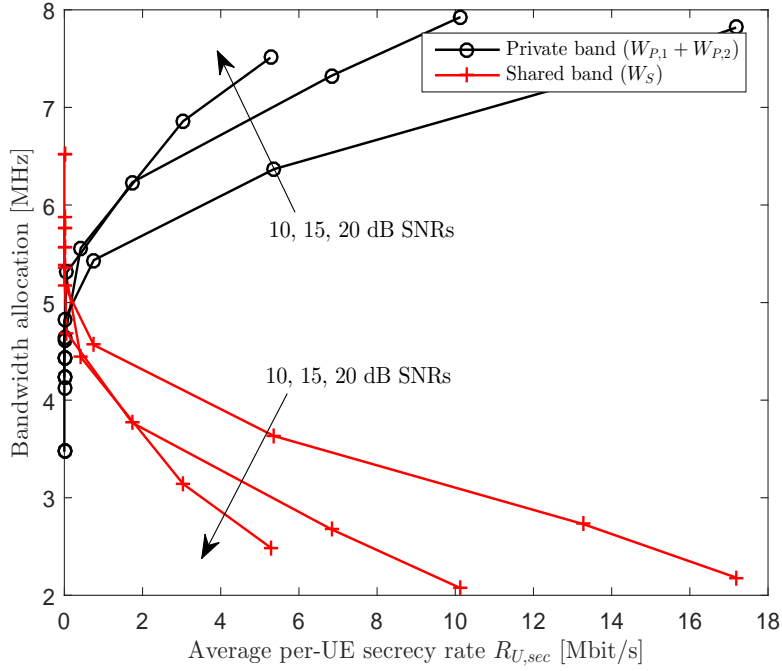
Figure 5. Bandwidth allocation versus average per-UE secrecy rate $R_{U,\text{sec}}$ ($N_R = N_U = 1$, $n_{R,i,r} = n_{U,i,k} = 1$, $C_{B,i} = 100$ Mbit/s, $C_{F,i,r} = 50$ Mbit/s and $W = 10$ MHz).

overall transmission rate, including both secure and insecure data streams.

Fig. 4 plots the average per-UE rate R_U versus the average per-UE secrecy rate $R_{U,\text{sec}}$ for a multi-tenant C-RAN with $N_R = N_U = 1$, $n_{R,i,r} = n_{U,i,k} = 1$, $C_{B,i} = 100$ Mbit/s, $C_{F,i,r} = 50$ Mbit/s, $W = 10$ MHz and 10, 15 and 20 dB signal-to-noise ratios (SNRs). The curves are obtained by varying the privacy threshold levels ranging from 5 Mbit/s to 60 Mbit/s in the constraints (23f). In the figure, the multi-tenant C-RAN system with the proposed optimization achieves a significantly improved rate-privacy trade-off as compared to the other two strategies with no spectrum pooling or uniform spectrum allocation. The gain becomes more significant at lower SNR levels, since the impact of inter-operator cooperation in the shared subband is more pronounced in this regime. As an example, in order to guarantee the per-UE secrecy rate of 2 Mbit/s, the proposed multi-tenant C-RAN system achieves a gain of about 69% gain in terms of per-UE rates at 10 dB SNR with respect to the traditional C-RAN system without spectrum pooling.

Fig. 5 plots the average bandwidth allocation between the private and shared subbands versus
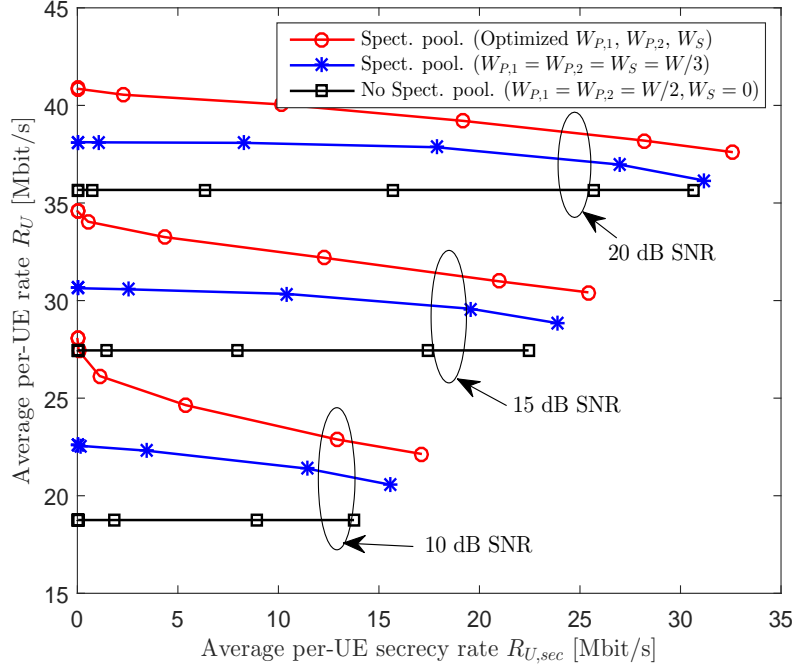
Figure 6. Average per-UE rate R_U versus average per-UE secrecy rate $R_{U,\text{sec}}$ ($N_R = N_U = 1$, $n_{R,i,r} = n_{U,i,k} = 2$, $C_{B,i} = 100$ Mbit/s, $C_{F,i,r} = 50$ Mbit/s and $W = 10$ MHz).

the average per-UE secrecy rate $R_{U,\text{sec}}$ for the set-up considered in Fig. 4. Consistently with the discussion above, as the SNR decreases, it is seen that more spectrum resources are allocated to the shared subband in order to leverage the opportunity of inter-operator cooperation.

In Fig. 6, we elaborate on the effect of the number of antennas. To this end, we show the average per-UE rate R_U versus the average per-UE secrecy rate $R_{U,\text{sec}}$ for a multi-tenant C-RAN with the same set-up discussed above except for $n_{R,i,r} = n_{U,i,k} = 2$ instead of $n_{R,i,r} = n_{U,i,k} = 1$. We can see that, compared to the single-antenna case, all the three schemes become more robust to the privacy constraint with the increased number of RU and UE antennas. This is due to the additional degrees of freedom in the precoding design that is afforded by the larger number of antennas.

We now study the impact of correlating the quantization noise signals across the RUs of operators by means of the multivariate compression strategy proposed in Sec. V. In Fig. 7(a), we plot the average per-UE rate R_U versus the average per-UE secrecy rate $R_{U,\text{sec}}$ for the same multi-tenant C-RAN set-up considered in Fig. 4 assuming spectrum pooling with optimized bandwidths
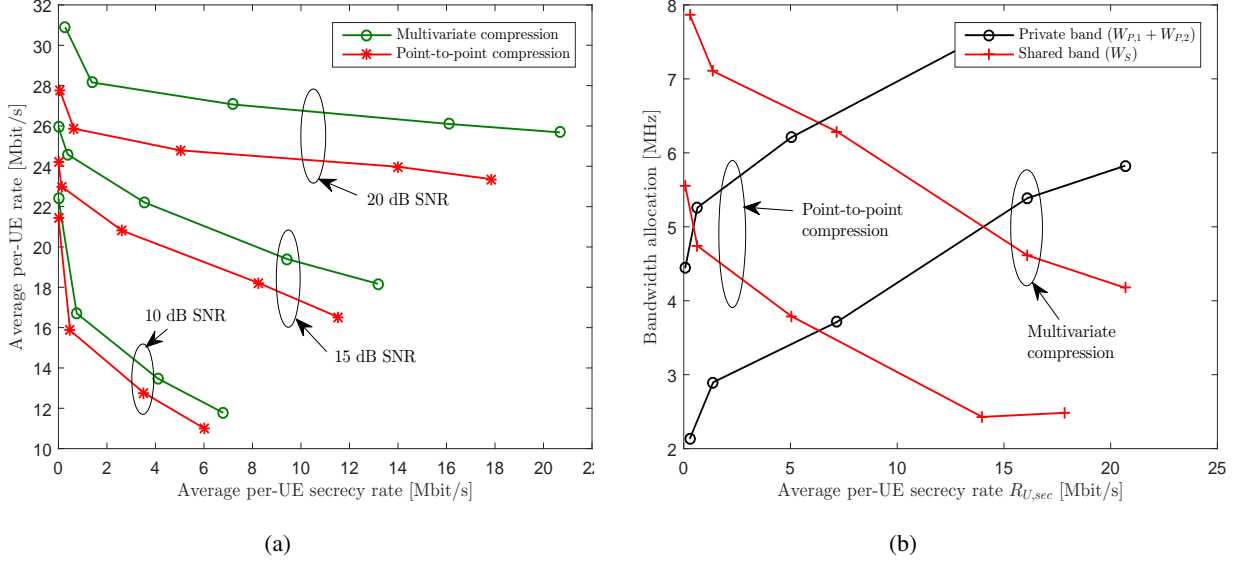
Figure 7. (a) Average per-UE rate R_U and (b) bandwidth allocation versus average per-UE secrecy rate $R_{U,\text{sec}}$ ($N_R = N_U = 1$, $n_{R,i,r} = n_{U,i,k} = 1$, $C_{B,i} = 100$ Mbit/s, $C_{F,i,r} = 50$ Mbit/s and $W = 10$ MHz).

$\{W_{P,1}, W_{P,2}, W_S\}$. We observe that multivariate compression is instrumental in improving the trade-off between inter-operator cooperation and privacy. The accrued performance gain increases with the SNR, since the performance degradation due to quantization is masked by the additive noise when the SNR is small. Fig. 7(b) plots the optimized bandwidth allocation versus the average per-UE secrecy rate $R_{U,\text{sec}}$ for a 20 dB SNR. The figure suggests that, with multivariate compression, it is desirable to allocate more bandwidth to the shared subband, given the added benefits of inter-operator cooperation in the presence of multivariate compression.

VII. Conclusions

In this work, we have studied the design of multi-tenant C-RAN systems with spectrum pooling under inter-operator privacy constraints. Assuming the standard C-RAN operation with quantized baseband signals, we first considered the standard point-to-point compression strategy, and then proposed a novel multivariate compression to achieve a better trade-off between the inter-operator cooperation and privacy. For both cases, we tackled the joint optimization of the bandwidth allocation among the private and shared subbands and of the precoding and fronthaul/backhaul compression strategies while satisfying constraints on fronthaul and backhaul capacity, per-RU transmit power and inter-operator privacy levels. To tackle the non-convex optimization problems, we converted the problems into DC problems with rank relaxation and

derived iterative algorithms based on the standard CCCP. We provided extensive numerical results to validate the effectiveness of the multi-tenant C-RAN system with the proposed optimization algorithm and multivariate compression. Among open problems, we mention the extension of the design and analysis to models with RAN sharing at the level of RUs and the consideration of hierarchical fog architectures.

APPENDIX A

By relaxing the non-convex rank constraints $\mathrm{rank}(\tilde{\mathbf{V}}_{i,k}^{(i)}) \le d_{i,k,P}$ and $\mathrm{rank}(\tilde{\mathbf{U}}_{i,k}^{(S)}) \le d_{i,k,S}$ explained in Sec. IV, the problem (23) can be converted into the DC problem

$$\underset{\substack{\tilde{\mathbf{V}}, \tilde{\mathbf{U}}, \mathbf{\Omega}, \mathbf{\Sigma}, \mathbf{W}, \\ \mathbf{R}, \mathbf{t}, \tilde{\mathbf{g}}, \tilde{\boldsymbol{\gamma}}, \tilde{\mathbf{p}}}}{\mathrm{maximize}} \sum_{i \in \mathcal{N}_O} \sum_{k \in \mathcal{N}_U} (R_{i,k,P} + R_{i,k,S}) \tag{31a}$$

$$\text{s.t.} \ \log R_{i,k,P} \le \log W_{P,i} + \log t_{f,i,k,P}, \ i \in \mathcal{N}_O, \ k \in \mathcal{N}_U, \tag{31b}$$

$$t_{f,i,k,P} \le f_{i,k,P}\left(\tilde{\mathbf{V}}, \mathbf{\Omega}\right), \ i \in \mathcal{N}_O, \ k \in \mathcal{N}_U, \tag{31c}$$

$$\log R_{i,k,S} \le \log W_S + \log t_{f,i,k,S}, \ i \in \mathcal{N}_O, \ k \in \mathcal{N}_U, \tag{31d}$$

$$t_{f,i,k,S} \le f_{i,k,S}\left(\tilde{\mathbf{V}}, \tilde{\mathbf{U}}, \mathbf{\Omega}\right) \ i \in \mathcal{N}_O, \ k \in \mathcal{N}_U, \tag{31e}$$

$$\sum_{m \in \{i,S\}} \tilde{g}_{i,r}^{(m)} + \tilde{\gamma}_{i,r}^{(S)} \le C_{F,i,r}, \ i \in \mathcal{N}_O, \ r \in \mathcal{N}_R, \tag{31f}$$

$$\log W_{i,m} + \log t_{g,i,r,m} \le \log \tilde{g}_{i,r}^{(m)}, \ i \in \mathcal{N}_O, \ r \in \mathcal{N}_R, \ m \in \{i,S\}, \tag{31g}$$

$$g_{i,r}^{(i)}\left(\tilde{\mathbf{V}}, \mathbf{\Omega}\right) \le t_{g,i,r,i}, \ i \in \mathcal{N}_O, \ r \in \mathcal{N}_R, \tag{31h}$$

$$g_{i,r}^{(S)}\left(\tilde{\mathbf{U}}, \mathbf{\Omega}\right) \le t_{g,i,r,S}, \ i \in \mathcal{N}_O, \ r \in \mathcal{N}_R, \tag{31i}$$

$$\log W_S + \log t_{\gamma,i,r,S} \le \log \tilde{\gamma}_{i,r}^{(S)}, \ i \in \mathcal{N}_O, \ r \in \mathcal{N}_R, \tag{31j}$$

$$\gamma_{i,r}^{(S)}\left(\tilde{\mathbf{U}}, \mathbf{\Sigma}\right) \le t_{\gamma,i,r,S}, \ i \in \mathcal{N}_O, \ r \in \mathcal{N}_R, \tag{31k}$$

$$\sum_{r \in \mathcal{N}_R} \tilde{\gamma}_{i,r}^{(S)} \le C_{B,i}, \ i \in \mathcal{N}_O, \tag{31l}$$

$$\log W_S + \log t_{\beta,i,k,S} \le \log \Gamma_{\mathrm{privacy}}, \ i \in \mathcal{N}_O, \ k \in \mathcal{N}_U, \tag{31m}$$

$$\beta_{i,k,S}\left(\tilde{\mathbf{U}}, \mathbf{\Omega}\right) \le t_{\beta,i,k,S}, \ i \in \mathcal{N}_O, \ k \in \mathcal{N}_U, \tag{31n}$$

$$\tilde{p}_{i,r}^{(i)} + \tilde{p}_{i,r}^{(S)} \le P_{i,r}, \ i \in \mathcal{N}_O, \ r \in \mathcal{N}_R, \tag{31o}$$

$$\log W_{i,m} + \log t_{p,i,r,m} \le \log \tilde{p}_{i,r}^{(m)}, \ i \in \mathcal{N}_O, \ r \in \mathcal{N}_R, \ m \in \{i,S\}, \tag{31p}$$

$$p_{i,r}^{(m)}\left(\tilde{\mathbf{V}}, \tilde{\mathbf{U}}, \mathbf{\Omega}\right) \le t_{p,i,r,m}, \ i \in \mathcal{N}_O, \ r \in \mathcal{N}_R, \ m \in \{i,S\}, \tag{31q}$$

$$W_{P,1} + W_{P,2} + W_S = W. \tag{31r}$$

Furthermore, at Step 2 in Algorithm 1, the CCCP approach solves the convex problem obtained

by linearizing the terms that induce non-convexity of problem (31). This can be written as

$$\underset{\substack{\tilde{\mathbf{V}}, \tilde{\mathbf{U}}, \boldsymbol{\Omega}, \boldsymbol{\Sigma}, \mathbf{W}, \\ \mathbf{R}, \mathbf{t}, \tilde{\mathbf{g}}, \tilde{\boldsymbol{\gamma}}, \tilde{\mathbf{p}}}}{\text{maximize}} \sum_{i \in \mathcal{N}_O} \sum_{k \in \mathcal{N}_U} (R_{i,k,P} + R_{i,k,S}) \tag{32a}$$

$$\text{s.t.} \ \varphi\left(R_{i,k,P}, R'_{i,k,P}\right) \le \log W_{P,i} + \log t_{f,i,k,P}, \ i \in \mathcal{N}_O, \ k \in \mathcal{N}_U, \tag{32b}$$

$$t_{f,i,k,P} \le \hat{f}_{i,k,P}\left(\tilde{\mathbf{V}}, \boldsymbol{\Omega}, \tilde{\mathbf{V}}', \boldsymbol{\Omega}'\right), \ i \in \mathcal{N}_O, \ k \in \mathcal{N}_U, \tag{32c}$$

$$\varphi\left(R_{i,k,S}, R'_{i,k,S}\right) \le \log W_S + \log t_{f,i,k,S}, \ i \in \mathcal{N}_O, \ k \in \mathcal{N}_U, \tag{32d}$$

$$t_{f,i,k,S} \le \hat{f}_{i,k,S}\left(\tilde{\mathbf{V}}, \tilde{\mathbf{U}}, \boldsymbol{\Omega}, \tilde{\mathbf{V}}', \tilde{\mathbf{U}}', \boldsymbol{\Omega}'\right) \ i \in \mathcal{N}_O, \ k \in \mathcal{N}_U, \tag{32e}$$

$$\sum_{m \in \{i,S\}} \tilde{g}_{i,r}^{(m)} + \tilde{\gamma}_{i,r}^{(S)} \le C_{F,i,r}, \ i \in \mathcal{N}_O, \ r \in \mathcal{N}_R, \tag{32f}$$

$$\varphi\left(W_{i,m}, W'_{i,m}\right) + \varphi\left(t_{g,i,r,m}, t'_{g,i,r,m}\right) \le \log \tilde{g}_{i,r}^{(m)}, \ i \in \mathcal{N}_O, \ r \in \mathcal{N}_R, \ m \in \{i, S\}, \tag{32g}$$

$$\hat{g}_{i,r}^{(i)}\left(\tilde{\mathbf{V}}, \boldsymbol{\Omega}, \tilde{\mathbf{V}}', \boldsymbol{\Omega}'\right) \le t_{g,i,r,i}, \ i \in \mathcal{N}_O, \ r \in \mathcal{N}_R, \tag{32h}$$

$$\hat{g}_{i,r}^{(S)}\left(\tilde{\mathbf{U}}, \boldsymbol{\Omega}, \tilde{\mathbf{U}}', \boldsymbol{\Omega}'\right) \le t_{g,i,r,S}, \ i \in \mathcal{N}_O, \ r \in \mathcal{N}_R, \tag{32i}$$

$$\varphi\left(W_S, W'_S\right) + \varphi\left(t_{\gamma,i,r,S}, t'_{\gamma,i,r,S}\right) \le \log \tilde{\gamma}_{i,r}^{(S)}, \ i \in \mathcal{N}_O, \ r \in \mathcal{N}_R, \tag{32j}$$

$$\hat{\gamma}_{i,r}^{(S)}\left(\tilde{\mathbf{U}}, \boldsymbol{\Sigma}, \tilde{\mathbf{U}}', \boldsymbol{\Sigma}'\right) \le t_{\gamma,i,r,S}, \ i \in \mathcal{N}_O, \ r \in \mathcal{N}_R, \tag{32k}$$

$$\sum_{r \in \mathcal{N}_R} \tilde{\gamma}_{\bar{i},r}^{(S)} \le C_{B,i}, \ i \in \mathcal{N}_O, \tag{32l}$$

$$\varphi\left(W_S, W'_S\right) + \varphi\left(t_{\beta,i,k,S}, t'_{\beta,i,k,S}\right) \le \log \Gamma_{\text{privacy}}, \ i \in \mathcal{N}_O, \ k \in \mathcal{N}_U, \tag{32m}$$

$$\hat{\beta}_{i,k,S}\left(\tilde{\mathbf{U}}, \boldsymbol{\Omega}, \tilde{\mathbf{U}}', \boldsymbol{\Omega}'\right) \le t_{\beta,i,k,S}, \ i \in \mathcal{N}_O, \ k \in \mathcal{N}_U, \tag{32n}$$

$$\tilde{p}_{i,r}^{(i)} + \tilde{p}_{i,r}^{(S)} \le P_{i,r}, \ i \in \mathcal{N}_O, \ r \in \mathcal{N}_R, \tag{32o}$$

$$\varphi\left(W_{i,m}, W'_{i,m}\right) + \varphi\left(t_{p,i,r,m}, t'_{p,i,r,m}\right) \le \log \tilde{p}_{i,r}^{(m)}, \ i \in \mathcal{N}_O, \ r \in \mathcal{N}_R, \ m \in \{i, S\}, \tag{32p}$$

$$p_{i,r}^{(m)}\left(\tilde{\mathbf{V}}, \tilde{\mathbf{U}}, \boldsymbol{\Omega}\right) \le t_{p,i,r,m}, \ i \in \mathcal{N}_O, \ r \in \mathcal{N}_R, \ m \in \{i, S\}, \tag{32q}$$

$$W_{P,1} + W_{P,2} + W_S = W, \tag{32r}$$

where we defined the functions

$$\hat{f}_{i,k,P}\left(\tilde{\mathbf{V}},\boldsymbol{\Omega},\tilde{\mathbf{V}}',\boldsymbol{\Omega}'\right) = \log_2 \det\left(\sum_{l\in\mathcal{N}_U}\mathbf{H}_{i,k}^i\tilde{\mathbf{V}}_{i,l}^{(i)}\mathbf{H}_{i,k}^{i\dagger} + \mathbf{H}_{i,k}^i\boldsymbol{\Omega}_i^{(i)}\mathbf{H}_{i,k}^{i\dagger} + \mathbf{I}\right) \tag{33}$$

$$-\frac{1}{\ln 2}\varphi\left(\begin{array}{c}\sum_{l\in\mathcal{N}_U\backslash\{k\}}\mathbf{H}_{i,k}^i\tilde{\mathbf{V}}_{i,l}^{(i)}\mathbf{H}_{i,k}^{i\dagger}+\mathbf{H}_{i,k}^i\boldsymbol{\Omega}_i^{(i)}\mathbf{H}_{i,k}^{i\dagger}+\mathbf{I},\\ \sum_{l\in\mathcal{N}_U\backslash\{k\}}\mathbf{H}_{i,k}^i\tilde{\mathbf{V}}_{i,l}^{(i)\prime}\mathbf{H}_{i,k}^{i\dagger}+\mathbf{H}_{i,k}^i\boldsymbol{\Omega}_i^{(i)\prime}\mathbf{H}_{i,k}^{i\dagger}+\mathbf{I}\end{array}\right),$$

$$\hat{f}_{i,k,S}\left(\tilde{\mathbf{V}},\tilde{\mathbf{U}},\boldsymbol{\Omega},\tilde{\mathbf{V}}',\tilde{\mathbf{U}}',\boldsymbol{\Omega}'\right) = \log_2 \det\left(\begin{array}{c}\sum_{l\in\mathcal{N}_U}\mathbf{G}_{i,k}^i\tilde{\mathbf{U}}_{i,l}^{(S)}\mathbf{G}_{i,k}^{i\dagger}\\ +\sum_{l\in\mathcal{N}_U}\mathbf{G}_{i,k}^{\bar{i}}\tilde{\mathbf{U}}_{\bar{i},l}^{(S)}\mathbf{G}_{i,k}^{\bar{i}\dagger}\\ +\mathbf{H}_{i,k}^i\boldsymbol{\Omega}_i^{(S)}\mathbf{H}_{i,k}^{i\dagger}+\mathbf{H}_{i,k}^i\boldsymbol{\Sigma}_i^{(S)}\mathbf{H}_{i,k}^{i\dagger}\\ +\mathbf{H}_{i,k}^{\bar{i}}\boldsymbol{\Omega}_{\bar{i}}^{(S)}\mathbf{H}_{i,k}^{\bar{i}\dagger}+\mathbf{H}_{i,k}^{\bar{i}}\boldsymbol{\Sigma}_{\bar{i}}^{(S)}\mathbf{H}_{i,k}^{\bar{i}\dagger}+\mathbf{I}\end{array}\right) \tag{34}$$

$$-\frac{1}{\ln 2}\varphi\left(\begin{array}{c}\left(\begin{array}{c}\sum_{l\in\mathcal{N}_U\backslash\{k\}}\mathbf{G}_{i,k}^i\tilde{\mathbf{U}}_{i,l}^{(S)}\mathbf{G}_{i,k}^{i\dagger}\\ +\sum_{l\in\mathcal{N}_U}\mathbf{G}_{i,k}^{\bar{i}}\tilde{\mathbf{U}}_{\bar{i},l}^{(S)}\mathbf{G}_{i,k}^{\bar{i}\dagger}\\ +\mathbf{H}_{i,k}^i\boldsymbol{\Omega}_i^{(S)}\mathbf{H}_{i,k}^{i\dagger}+\mathbf{H}_{i,k}^i\boldsymbol{\Sigma}_i^{(S)}\mathbf{H}_{i,k}^{i\dagger}\\ +\mathbf{H}_{i,k}^{\bar{i}}\boldsymbol{\Omega}_{\bar{i}}^{(S)}\mathbf{H}_{i,k}^{\bar{i}\dagger}+\mathbf{H}_{i,k}^{\bar{i}}\boldsymbol{\Sigma}_{\bar{i}}^{(S)}\mathbf{H}_{i,k}^{\bar{i}\dagger}+\mathbf{I}\end{array}\right),\\ \left(\begin{array}{c}\sum_{l\in\mathcal{N}_U\backslash\{k\}}\mathbf{G}_{i,k}^i\tilde{\mathbf{U}}_{i,l}^{(S)\prime}\mathbf{G}_{i,k}^{i\dagger}\\ +\sum_{l\in\mathcal{N}_U}\mathbf{G}_{i,k}^{\bar{i}}\tilde{\mathbf{U}}_{\bar{i},l}^{(S)\prime}\mathbf{G}_{i,k}^{\bar{i}\dagger}\\ +\mathbf{H}_{i,k}^i\boldsymbol{\Omega}_i^{(S)\prime}\mathbf{H}_{i,k}^{i\dagger}+\mathbf{H}_{i,k}^i\boldsymbol{\Sigma}_i^{(S)\prime}\mathbf{H}_{i,k}^{i\dagger}\\ +\mathbf{H}_{i,k}^{\bar{i}}\boldsymbol{\Omega}_{\bar{i}}^{(S)\prime}\mathbf{H}_{i,k}^{\bar{i}\dagger}+\mathbf{H}_{i,k}^{\bar{i}}\boldsymbol{\Sigma}_{\bar{i}}^{(S)\prime}\mathbf{H}_{i,k}^{\bar{i}\dagger}+\mathbf{I}\end{array}\right)\end{array}\right),$$

$$\hat{g}_{i,r}^{(i)}\left(\tilde{\mathbf{V}},\boldsymbol{\Omega},\tilde{\mathbf{V}}',\boldsymbol{\Omega}'\right) = \frac{1}{\ln 2}\varphi\left(\sum_{k\in\mathcal{N}_U}\mathbf{E}_{i,r}^\dagger\tilde{\mathbf{V}}_{i,k}^{(i)}\mathbf{E}_{i,r}+\boldsymbol{\Omega}_{i,r}^{(i)},\sum_{k\in\mathcal{N}_U}\mathbf{E}_{i,r}^\dagger\tilde{\mathbf{V}}_{i,k}^{(i)\prime}\mathbf{E}_{i,r}+\boldsymbol{\Omega}_{i,r}^{(i)\prime}\right)$$

$$-\log_2 \det\left(\boldsymbol{\Omega}_{i,r}^{(i)}\right), \tag{35}$$

$$\hat{g}_{i,r}^{(S)}\left(\tilde{\mathbf{U}},\boldsymbol{\Omega},\tilde{\mathbf{U}}',\boldsymbol{\Omega}'\right) = \frac{1}{\ln 2}\varphi\left(\sum_{k\in\mathcal{N}_U}\tilde{\mathbf{E}}_{i,r}^\dagger\tilde{\mathbf{U}}_{i,k}^{(S)}\tilde{\mathbf{E}}_{i,r}+\boldsymbol{\Omega}_{i,r}^{(S)},\sum_{k\in\mathcal{N}_U}\tilde{\mathbf{E}}_{i,r}^\dagger\tilde{\mathbf{U}}_{i,k}^{(S)\prime}\tilde{\mathbf{E}}_{i,r}+\boldsymbol{\Omega}_{i,r}^{(S)\prime}\right)$$

$$-\log_2 \det\left(\boldsymbol{\Omega}_{i,r}^{(S)}\right), \tag{36}$$

$$\hat{\gamma}_{i,r}^{(S)}\left(\tilde{\mathbf{U}},\boldsymbol{\Sigma},\tilde{\mathbf{U}}',\boldsymbol{\Sigma}'\right) = \frac{1}{\ln 2}\varphi\left(\sum_{k\in\mathcal{N}_U}\bar{\mathbf{E}}_{\bar{i},r}^\dagger\tilde{\mathbf{U}}_{\bar{i},k}^{(S)}\bar{\mathbf{E}}_{\bar{i},r}+\boldsymbol{\Sigma}_{i,r}^{(S)},\sum_{k\in\mathcal{N}_U}\bar{\mathbf{E}}_{\bar{i},r}^\dagger\tilde{\mathbf{U}}_{\bar{i},k}^{(S)\prime}\bar{\mathbf{E}}_{\bar{i},r}+\boldsymbol{\Sigma}_{i,r}^{(S)\prime}\right)$$

$$-\log_2 \det\left(\boldsymbol{\Sigma}_{i,r}^{(S)}\right), \tag{37}$$

$$\hat{\beta}_{i,k,S}\left(\tilde{\mathbf{U}},\boldsymbol{\Omega},\tilde{\mathbf{U}}',\boldsymbol{\Omega}'\right) = \frac{1}{\ln 2}\varphi\left(\sum_{l\in\mathcal{N}_U}\bar{\mathbf{E}}_i^\dagger\tilde{\mathbf{U}}_{i,k}^{(S)}\bar{\mathbf{E}}_i+\boldsymbol{\Sigma}_{\bar{i}}^{(S)},\sum_{l\in\mathcal{N}_U}\bar{\mathbf{E}}_i^\dagger\tilde{\mathbf{U}}_{i,k}^{(S)\prime}\bar{\mathbf{E}}_i+\boldsymbol{\Sigma}_{\bar{i}}^{(S)\prime}\right)$$

$$-\log_2 \det\left(\sum_{l\in\mathcal{N}_U\backslash\{k\}}\bar{\mathbf{E}}_i^\dagger\tilde{\mathbf{U}}_{i,k}^{(S)}\bar{\mathbf{E}}_i+\boldsymbol{\Sigma}_{\bar{i}}^{(S)}\right). \tag{38}$$

with the notations $\varphi(\mathbf{A}, \mathbf{B}) = \ln\det(\mathbf{B}) + \mathrm{tr}(\mathbf{B}^{-1}(\mathbf{A}-\mathbf{B}))$, $\mathbf{G}_{i,k}^{j} = [\mathbf{H}_{i,k}^{j}\ \mathbf{H}_{i,k}^{\bar{j}}]$, $\tilde{\mathbf{E}}_{i,r} = [\mathbf{E}_{i,r}^{\dagger}\ \mathbf{0}_{n_{R,\bar{i}} \times n_{R,i,r}}^{\dagger}]^{\dagger}$, $\bar{\mathbf{E}}_{i,r} = [\mathbf{0}_{n_{R,i} \times n_{R,\bar{i},r}}^{\dagger}\ \mathbf{E}_{\bar{i},r}^{\dagger}]^{\dagger}$ and $\bar{\mathbf{E}}_{i} = [\mathbf{0}_{n_{R,i} \times n_{R,\bar{i}}}^{\dagger}\ \mathbf{I}_{n_{R,\bar{i}}}]^{\dagger}$.

References

[1] A. Khan, W. Kellerer, K. Kozu and M. Yabusaki, "Network sharing in the next mobile network: TCO reduction, management flexibility, and operational independence," *IEEE Commn. Mag.*, vol. 49, no. 10, pp. 134-142, Oct. 2011.

[2] E. A. Jorswieck, L. Badia, T. Fahldieck, E. Karipidis and J. Luo, "Spectrum sharing improves the network efficiency for cellular operators," *IEEE Commun. Mag.*, vol. 52, no. 3, pp. 129-136, Mar. 2014.

[3] K. Samdanis, X. Costa-Perez and V. Sciancalepore, "From network sharing to multi-tenancy: The 5G network slicer broker," *IEEE Commun. Mag.*, vol. 54, no. 7, pp. 32-39, Jul. 2016.

[4] F. Boccardi, H. Shorkri-Ghadikolaei, G. Fodor, E. Erkip, G. Fischione, M. Kountouris, P. Popovski and M. Zorzi, "Spectrum pooling in mmWave networks: Opportunities, challenges, and enablers," *IEEE Commun. Mag.*, vol. 54, no. 11, pp. 33-39, Nov. 2016.

[5] O. Aydin, E. A. Jorswieck, D. Aziz and A. Zappone, "Energy-spectral efficiency tradeoffs in 5G multi-operator networks with heterogeneous constraints," *IEEE Trans. Wireless Comm.*, vol. 16, no. 9, pp. 5869-5881, Sep. 2017.

[6] J. Park, J. G. Andrews and R. W. Heath Jr., "Inter-operator base station coordination in spectrum-shared millimeter wave cellular networks," arXiv:1709.06239, Sep. 2017.

[7] X. Foukas, G. Patounas, A. Elmokashfi and M. K. Marina, "Network slicing in 5G: Survey and challenges," *IEEE Comm. Mag.*, vol. 55, no. 5, pp. 94-100, May 2017.

[8] O. Simeone, A. Maeder, M. Peng, O. Sahin and W. Yu, "Cloud radio access network: Virtualizing wireless access for dense heterogeneous systems," *Journ. Comm. Networks*, vol. 18, no. 2, pp. 135-149, Apr. 2016.

[9] T. Q. Quek, M. Peng, O. Simeone and W. Yu, *Cloud Radio Access Networks: Principles, Technologies, and Applications*, Cambridge Univ. Press, Apr. 2017.

[10] O. Simeone, O. Somekh, H. V. Poor and S. Shamai (Shitz), "Downlink multicell processing with limited-backhaul capacity," *EURASIP J. Adv. Sig. Proc.*, 2009.

[11] S.-H. Park, O. Simeone, O. Sahin and S. Shamai (Shitz), "Joint precoding and multivariate backhaul compression for the downlink of cloud radio access networks," *IEEE Trans. Sig. Processing*, vol. 61, no. 22, pp. 5646-5658, Nov. 2013.

[12] S.-H. Park, O. Simeone, O. Sahin and S. Shamai (Shitz), "Fronthaul compression for cloud radio access networks: Signal processing advances inspired by network information theory," *IEEE Sig. Proc. Mag.*, vol. 31, no. 6, pp. 69-79, Nov. 2014.

[13] M. Tao, E. Chen, H. Zhou and W. Yu, "Content-centric sparse multicast beamforming for cache-enabled cloud RAN," *IEEE Trans. Wireless Comm.*, vol. 15, no. 9, pp. 6118-6131, Sep. 2016.

[14] W. Lee, O. Simeone, J. Kang and S. Shamai (Shitz), "Multivariate fronthaul quantization for downlink C-RAN," *IEEE Trans. Sig. Proc.*, vol. 64, no. 19, pp. 5025-5037, Oct. 2016.

[15] S.-H. Park, O. Simeone and S. Shamai (Shitz), "Joint optimization of cloud and edge processing for fog radio access networks," *IEEE Trans. Wireless Comm.*, vol. 15, no. 11, pp. 7621-7632, Nov. 2016.

[16] L. Liu and W. Yu, "Cross-layer design for downlink multihop cloud radio access networks with network coding," *IEEE Trans. Sig. Proc.*, vol. 65, no. 7, pp. 1728-1740, Apr. 2017.

[17] S.-H. Park, O. Simeone, O. Sahin and S. Shamai (Shitz), "Robust and efficient distributed compression for cloud radio access networks," *IEEE Trans. Veh. Tech.*, vol. 62, no. 2, pp. 692-703, Feb. 2013.

[18] Y. Zhou, Y. Xu, W. Yu and J. Chen, "On the optimal fronthaul compression and decoding strategies for uplink cloud radio access networks," *IEEE Trans. Inf. Theory*, vol. 62, no. 2, pp. 7402-7418, Dec. 2016.

[19] X. He and A. Yener, "Cooperation with an untrusted realy: A secrecy perspective," *IEEE Trans. Inf. Theory*, vol. 56, no. 8, pp. 3807-3827, Aug. 2010.

[20] R. Bassily, E. Ekrem, X. He, E. Tekin, J. Xie, M. R. Bloch, S. Ulukus and A. Yener, "Cooperative security at the physical layer," *IEEE Sig. Proc. Mag.*, vol. 30, no. 5, pp. 16-28, Sep. 2013.

[21] J. Ostergaard and R. Zamir, "Multiple-description coding by dithered delta-sigma quantization," *IEEE Trans. Inf. Theory*, vol. 55, no. 10, pp. 4661-4675, Oct. 2009.

[22] A. E. Gamal and Y.-H. Kim, *Network Information Theory*, Cambridge University Press, 2011.

[23] I. Csiszar and J. K. Korner, *Information Theory: Coding Theorems for Discrete Memoryless Systems*, Academic Press, London, 1981.

[24] M. Grant and S. Boyd, "CVX: Matlab software for disciplined convex programming," ver 2.0 beta, Sep. 2013. [Online]. Available: http://cvxr.com/cvx.